

# UC Irvine

## UC Irvine Previously Published Works

### Title

Rotational multiphoton endoscopy with a 1 microm fiber laser system.

### Permalink

<https://escholarship.org/uc/item/64f0f9t2>

### Journal

Optics Letters, 34(15)

### ISSN

0146-9592

### Authors

Liu, Gangjun  
Xie, Tuqiang  
Tomov, Ivan V  
et al.

### Publication Date

2009-08-01

### DOI

10.1364/ol.34.002249

### Copyright Information

This work is made available under the terms of a Creative Commons Attribution License, available at <https://creativecommons.org/licenses/by/4.0/>

Peer reviewed

Published in final edited form as:

*Opt Lett.* 2009 August 1; 34(15): 2249–2251.

## Rotational multiphoton endoscopy with a 1 $\mu\text{m}$ fiber laser system

Gangjun Liu<sup>1</sup>, Tuqiang Xie<sup>1</sup>, Ivan V. Tomov<sup>1</sup>, Jianping Su<sup>2</sup>, Lingfeng Yu<sup>2</sup>, Jun Zhang<sup>1</sup>, Bruce J. Tromberg<sup>1</sup>, and Zhongping Chen<sup>1,2,\*</sup>

<sup>1</sup> Beckman Laser Institute, University of California, Irvine, Irvine, California 92612, USA

<sup>2</sup> Department of Biomedical Engineering, University of California, Irvine, Irvine, California 92617, USA

### Abstract

We present multiphoton microendoscopy with a rotational probe and a 1  $\mu\text{m}$  fiber-based femtosecond laser. The rotational probe is based on a double-clad photonic crystal fiber, a gradient index lens, a microprism, and a rotational microelectromechanical system (MEMS) motor. The MEMS motor has a diameter of 2.2 mm and can provide 360° full-view rotation. The fiber laser provides ultrashort pulses with a central wavelength at 1.034  $\mu\text{m}$  and a repetition rate of 50 MHz. Second-harmonic-generation images of rat-tail tendon and fish scale are demonstrated with the rotational probe-based multiphoton system.

---

Multiphoton optical microscopy (MPM) is a powerful tool in the imaging sciences. Compared with their linear counterpart, MPM allows deeper penetration into thick tissues owing to near-IR excitation wavelength used [1]. Because the excitation is confined to the focal region in MPM, out-of-focus photobleaching and photodamage is greatly reduced [1]. Since the introduction of MPM, these tools have been widely used in the fields of biological and medical sciences.

Commercially available femtosecond Ti:sapphire lasers are the most commonly used laser sources for MPM. Ti:sapphire lasers are broadly tunable from 700 to 1000 nm. A longer wavelength source beyond 1  $\mu\text{m}$  is also of interest. At longer excitation wavelengths, penetration depth is greater owing to reduced scattering coefficient at a longer excitation wavelength [2]. When shifting the excitation wavelength from 800 to 1000 nm and keeping the other factors the same, imaging depth will be increased greatly for tissues such as skin, muscle, and tumor [2]. A 1.3  $\mu\text{m}$  source may improve the imaging depth twofold as compared with a conventional 800 nm source [3]. Fiber lasers may operate at 1.0, 1.3, and 1.5  $\mu\text{m}$  [2]. With the light confined in fiber, fiber-based sources are more compact and not susceptible to misalignment. Fiber-based sources with fiber output allow direct coupling with a fiber-based system.

Miniaturization of the nonlinear microscopy is of great interest for imaging tissues *in vivo* and *ex vivo*. The challenges for the miniaturization are efficient excitation pulse delivery with minimal pulse distortion, efficient multiphoton signal collection, and miniature scanning mechanism. Various fibers, including single-mode fiber, hollow core fiber, fiber bundle, and double-clad photonic crystal fiber (DCPCF), have been investigated for MPM endoscopy applications [4–8]. Of these, the DCPCF is unique because it can support single-mode propagation of the excitation wavelength through a relatively large area core while

---

\*Corresponding author: z2chen@uci.edu.

simultaneously supporting the multimode propagation of the multiphoton signal through the high-NA inner clad [6,8]. The relatively large-area core can significantly reduce the power density in the core and, therefore, minimize the nonlinear effects. The clad has a large diameter with a high NA, and high signal collection efficiency can be achieved [6,8]. For the scanning mechanism, two-axis micro-electromechanical system (MEMS) scanning mirror, piezoelectric, and electromagnetic actuators have been proposed to scan the laser beam [4,8–11]. The piezoelectric and electromagnetic actuators provide a forward spiral or Lissajous scan pattern, and the MEMS mirrors provide two axes scanning from a sideview direction.

For biomedical imaging applications such as the in-travascular and gastrointestinal tract, sideview rotational imaging is preferred owing to their hollow feature. In this Letter, we propose MPM that uses a rotational microprobe and a 1  $\mu\text{m}$  fiber laser. The rotational probe consists of a DCPCF, a gradient index (GRIN) lens, a microprism, and a rotational MEMS motor. The fiber laser produces ultrashort femtosecond pulses with a central wavelength at 1.034  $\mu\text{m}$ , a spectral width of 13 nm, and a repetition rate of 50 MHz. Two-dimensional beam scanning is realized by the linear transversal scanning provided by a linear stage and rotational scanning by an MEMS motor.

Our system setup is shown in Fig. 1. A home-built, mode-locked, self-starting, stretched-pulse, Yb-doped fiber laser generates ultrashort pulses with the central wavelength at 1.034  $\mu\text{m}$  and a repetition rate of 50 MHz [12]. The mode-locked pulses from the fiber oscillator are temporally stretched in a 10 m single-mode fiber and amplified in yttrium-doped fiber pumped by two 980 nm diode lasers. A polarized pulse with a maximum output power of 270 mW is obtained after dechirping by an external grating pair. Because most of the parts are fiber based in this laser, the entire laser source occupies a dimension of 30 cm  $\times$  45 cm  $\times$  12 cm, and it can be compacted into a much smaller space. Laser beam after the grating pair is coupled into a DCPCF (Crystal Fiber A/S, DC-165-16-PASSIVE) by a microscope objective. The output beam pattern from the DCPCF is monitored to guarantee the core mode operation. In our current configuration, the coupling efficiency of the excitation laser beam to the DCPCF is approximately 50%. More than 50% of the total output power going through the DCPCF is in the core of the fiber. The core mode power is measured by spatially filtering the light in the clad with an iris. The laser beam through the DCPCF is sent to a homemade interference autocorrelator to monitor the pulse width. By adjusting the distance between the grating pair and monitoring the interference autocorrelation trace of the output pulse, we get the shortest pulse through the DCPCF. The shortest pulse width through the DCPCF is 290 fs after dispersion compensation. The multiphoton signal collected by the DCPCF is separated from the input via a dichroic beam-splitter and then focused on a photomultiplier tube (PMT) after passing through a short-pass emission filter. Signal from the PMT is further amplified by a low-noise pre-amplifier (Stanford Research Systems, Inc., SR560) before being sent to a personal computer for data acquisition (DAQ) and processing.

For initially testing of the DCPCF and GRIN lens for the 1  $\mu\text{m}$  fiber laser system, we used a two-photon diode (Hamamatsu Photonics, G1115) as a sample and detected the two-photon signal versus the incident power. The two-photon diode has a spectral range of 300–680 nm, and its output was amplified by a low-noise-current preamplifier (Stanford Research Systems, Inc., SR570). The quadratic power dependence confirms the two-photon nature of the signal. To further test the excitation and signal collection efficiency of our system, we used potassium dihydrogen phosphate (KDP) crystal powder as a sample and tried to find the relationship between the excitation power and second-harmonic signal collected by the DCPCF. Figure 2 shows this relationship. The quadratic power dependence of the second-harmonic-generation (SHG) signal on the excitation power can be seen from the fitted curve.

We have developed a sideview imaging rotational probe for optical coherent tomography endoscopy [13]. However, to our knowledge this kind of probe has not been demonstrated in the nonlinear microscopy field. The schematic of the microrotational probe is illustrated in Fig. 3(a). Light passed through the DCPCF is focused by a GRIN lens. The focusing beam after the GRIN lens is reflected by a right-angle microprism glued to the shaft of the microrotational motor. The 1 mm microprism is coated with aluminum, and it provides more than 90% reflection efficiency. The MEMS rotational motor is 2.2 mm in diameter and 12 mm in length, including the shaft. The rotational motor is driven by an external motor controller through a control wire. The MEMS rotational motor can reach about 40 rounds/s without any load on the shaft. With the microprism glued to the shaft, the rotation speed drops to 5 rounds/s. The only moving part in this configuration is the microprism glued to the shaft of the MEMS motor. Figure 3(b) shows the photograph of the rotational MEMS motor glued with the microprism together with a United States dime coin.

Collagen is the main structural protein and fibrous component for tendon, skin, bone, and cartilage. Collagen may be highly ordered and possesses a large second-order nonlinear susceptibility. It is known that rat-tail tendon and fish scale consist of dense collagen fibrils, and they are expected to yield a bright SHG signal. In this study, the tail was removed from a rat sacrificed from another experiment and was frozen for hours before our experiment. The rat-tail tendon was removed from the thawed rat tail and imaged. Scales was plucked from live fish and kept at room temperature for hours before experiment. Figures 4(a) and 4(b) show the SHG images of the rat-tail tendon and the fish scale. The scale bar is 25  $\mu\text{m}$ . X-direction (horizontal direction in the picture) scanning is realized by the rotational probe. Y-direction scanning (vertical direction in the picture) is realized by a translation stage. Rotation speed of the MEMS motor is set at 1 round/s to enhance the contrast. The excitation power delivered on the sample is 50 mW (through the core of the fiber based on 50% of the total output power in the core). When processing the data, background noise is subtracted first. Background noise is determined by the DAQ signal without the sample. The background-noise-subtracted signal is expressed in eighth-bit pseudocolor according to the signal value. In the results shown here, we demonstrate only a 100  $\mu\text{m}$  imaging range in the rotation direction. The coated microprism could achieve a 360° full-circle view so the probe could realize 360° rotational imaging. The packaged probe could also be designed as a needle type for deep-tissue imaging.

In conclusion, we demonstrated a design of a rotational MPM probe and used a 1  $\mu\text{m}$  fiber laser as a laser source. The probe is based on a DCPCF, a GRIN lens, a microprism, and an MEMS motor. We experimentally verified the feasibility of the DCPCF fiber as signal delivery and multiphoton signal collection media for an MPM system with 1  $\mu\text{m}$  excitation wavelength. SHG images were demonstrated with the rotational probe and a fiber-laser-based MPM system. The probe can achieve a 360° full-circle view and could realize a deep-tissue, large-imaging range if packaged in a needle form.

## Acknowledgments

This work was supported by the National Institutes of Health (NIH) (EB-00293, NCI-91717, RR-01192), National Science Foundation (NSF) (BES-86924), Air Force Office of Scientific Research (AFOSR) (FA9550-04-0101), and the Beckman Laser Institute Endowment.

## References

1. Helmchen F, Denk W. Nat Med. 2005; 2:932.
2. Tromberg, BJ. Handbook of Biomedical Nonlinear Optical Microscopy. Masters, BR.; So, PTC., editors. Oxford: U. Press; 2008. p. 707-715.

3. Balu M, Baldacchini T, Carter J, Krasieva TB, Zadoyan R, Tromberg BJ. *J Biomed Opt.* 2009; 14:010508–1. [PubMed: 19256688]
4. Jung JC, Schnitzer MJ. *Opt Lett.* 2003; 28:902. [PubMed: 12816240]
5. Flusberg BA, Cocker ED, Piyawattanametha W, Jung JC, Cheung ELM, Schnitzer MJ. *Nat Med.* 2005; 2:941.
6. Myaing MT, Ye JY, Norris TB, Thomas T, Baker JR Jr, Wadsworth WJ, Bouwmans G, Knight JC, St Russell PJ. *Opt Lett.* 2003; 28:1224. [PubMed: 12885028]
7. Göbel W, Kerr JND, Nimmerjahn AL, Helmchen F. *Opt Lett.* 2004; 29:2521. [PubMed: 15584281]
8. Fu L, Gan X, Gu M. *Opt Express.* 2005; 13:5528. [PubMed: 19498549]
9. Jung W, Tang S, McCormic DT, Xie T, Ahn Y, Su J, Tomov IV, Krasieva TB, Tromberg BJ, Chen Z. *Opt Lett.* 2008; 33:1324. [PubMed: 18552946]
10. Myaing MT, MacDonald DJ, Li X. *Opt Lett.* 2006; 31:1076. [PubMed: 16625908]
11. Engelbrecht CJ, Johnston RS, Seibel EJ, Helmchen F. *Opt Express.* 2008; 16:5556. [PubMed: 18542658]
12. Lim H, Ilday FÖ, Wise FW. *Opt Lett.* 2003; 28:660. [PubMed: 12703933]
13. Su J, Zhang J, Yu L, Chen Z. *Opt Express.* 2007; 15:10390. [PubMed: 19547391]

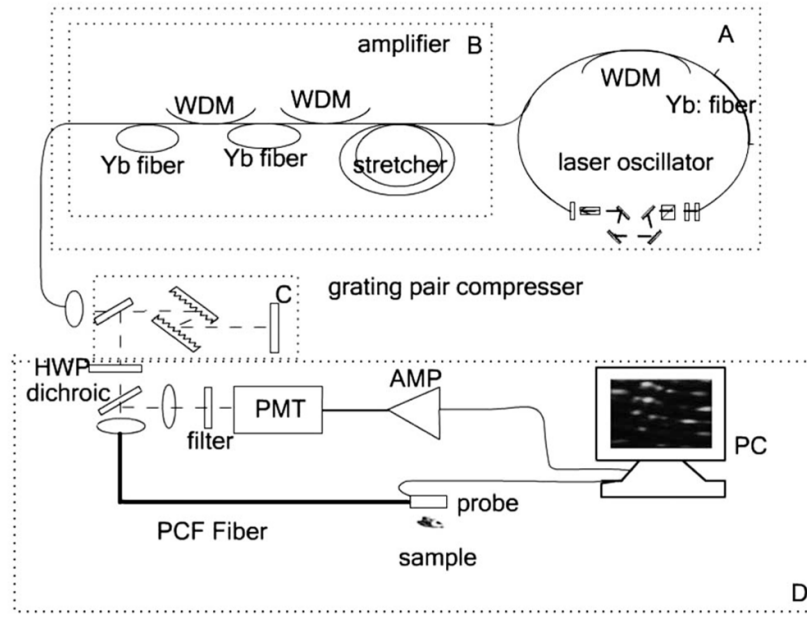


**Fig. 1.** Diagram of the multiphoton imaging system. A, fiber laser oscillator; B, fiber amplifier; C, grating pair compressor; D, the microprobe, data acquisition, and processing system. WDM, wavelength-division multiplexer; PCF, photonic crystal fiber; HWP, half-wave plate; PMT, photo-multiplier tube; AMP, amplifier.

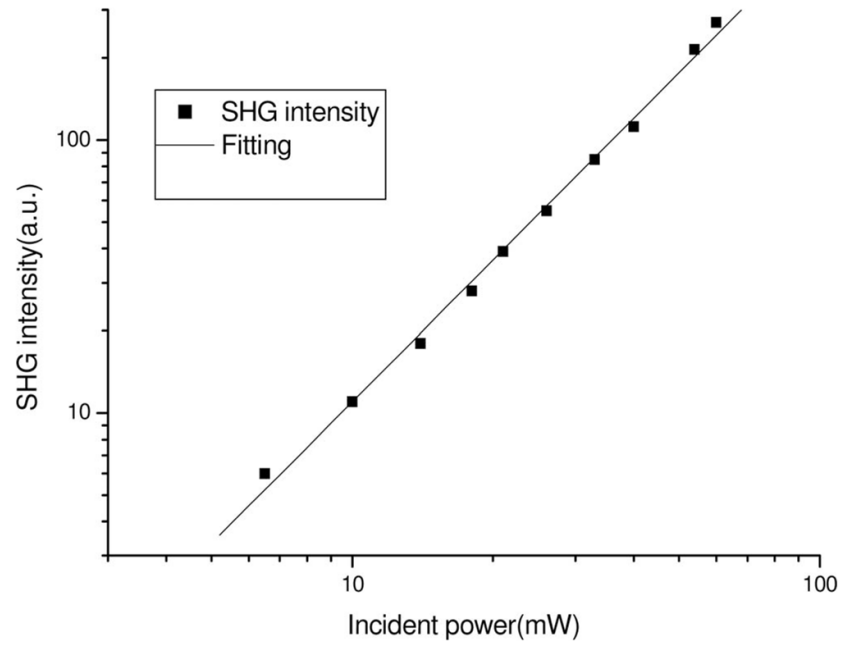


**Fig. 2.** Double-logarithmic plot of the SHG intensity from KDP crystal power as a function of incident power.

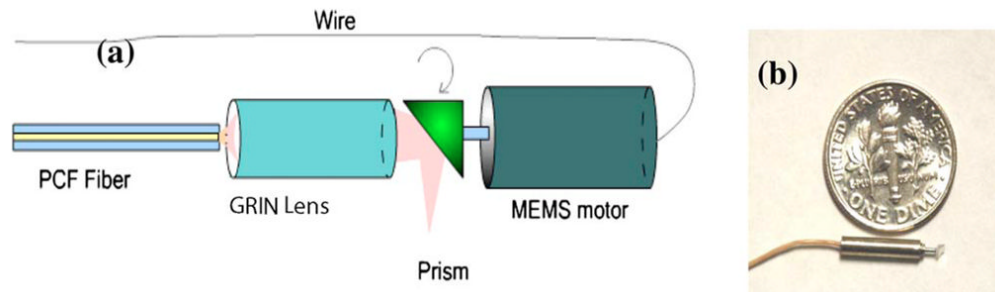


**Fig. 3.** (Color online) Diagram of the microrotational probe. The probe is based on a DCPCF, a GRIN lens, a microprism, and a rotational MEMS motor. (b) Photograph of the microprism glued to a MEMS motor together with a United States dime coin.



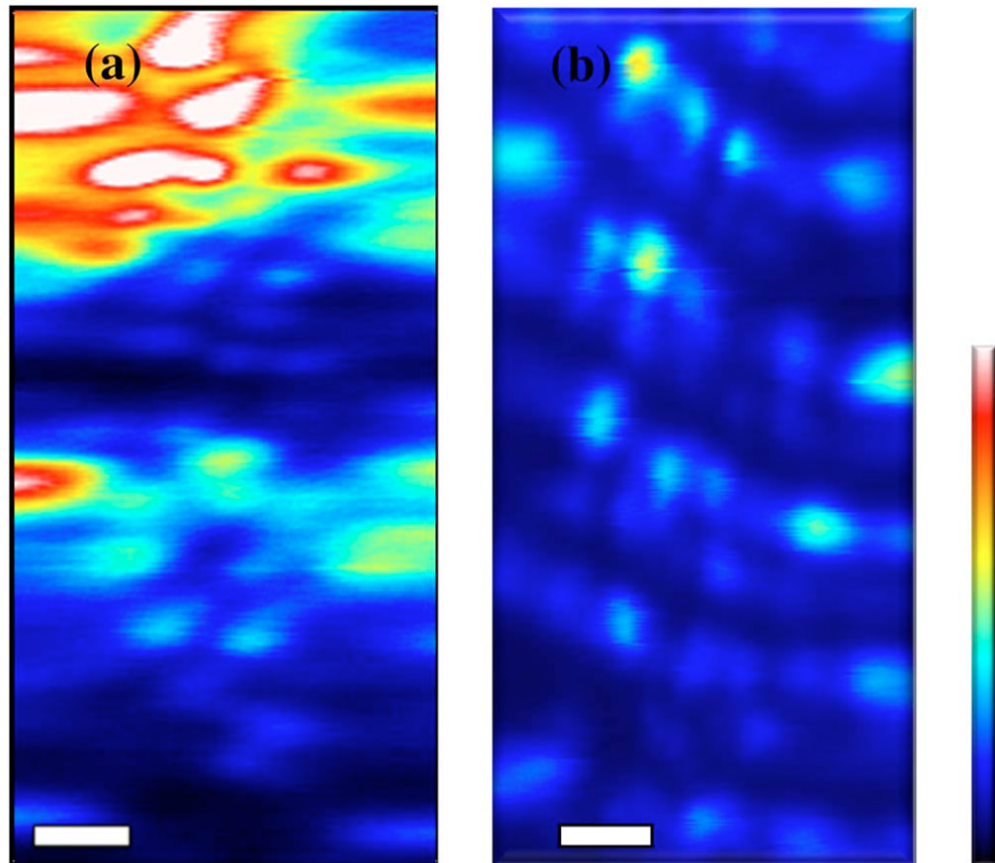


**Fig. 4.** (Color online) SHG images of (a) a rat tail tendon and (b) a fish scale. Scale bar is 25  $\mu\text{m}$ .